

**Key Points:**

- EURO-CORDEX verification over Iberian Peninsula
- Observational uncertainty analysis of the evaluation of the EURO-CORDEX RCMs
- Synoptic patterns and observational uncertainty of precipitation regimes

**Correspondence to:**

S. Herrera,  
 sexto.herrera@unican.es

**Citation:**

Herrera, S., Soares, P. M. M., Cardoso, R. M., & Gutierrez, J. M. (2020). Evaluation of the EURO-CORDEX regional climate models over the Iberian Peninsula: Observational uncertainty analysis. *Journal of Geophysical Research: Atmospheres*, 125, e2020JD032880. <https://doi.org/10.1029/2020JD032880>

Received 5 APR 2020

Accepted 27 MAY 2020

Accepted article online 29 MAY 2020

## Evaluation of the EURO-CORDEX Regional Climate Models Over the Iberian Peninsula: Observational Uncertainty Analysis

**S. Herrera<sup>1</sup> , P. M. M. Soares<sup>2</sup> , R. M. Cardoso<sup>2</sup> , and J. M. Gutiérrez<sup>3</sup>**

<sup>1</sup>Department of Applied Mathematics and Computer Science, Universidad de Cantabria, Santander, Spain, <sup>2</sup>Instituto Dom Luiz (IDL), Facultade de Ciencias, Universidade de Lisboa, Lisboa, Portugal, <sup>3</sup>Instituto de Física de Cantabria, CSIC-University of Cantabria, Santander, Spain

**Abstract** This work evaluates the daily precipitation and mean temperature of eight CORDEX-EUR11 ERA-Interim-driven simulations of EURO-CORDEX over the Iberian Peninsula (IP) for the period 1989–2008. To this aim, three observational data sets (Iberia01, E-OBS-v19e, and MESAN-0.11) were considered as reference and compared with the models by means of several indices reflecting the mean and extreme regimes over the IP. For precipitation the Lamb weather types were considered to identify synoptic conditions related with higher observational uncertainty. RCMs are able to reproduce the spatial pattern and the variability observed in the IP. However, there is a higher agreement between models and observations for mean temperature than for precipitation, decreasing when extremes are analyzed. For the observational uncertainty analysis, also extreme daily temperatures were considered to obtain a wider picture of this topic. A higher dependence on the observational data set has been found for precipitation than for temperature. This uncertainty is particularly significant when the 50-year return value is considered for which the observational uncertainty doubles the model uncertainty. Only the wet-day frequency presents values lower than 0.5 for all seasons, with most of the rest of values reflecting a similar contribution of both components to the uncertainty. In the case of temperatures, the main contribution of the observations has been found when the lower (MAE01) and upper (MAE99) extremes are considered, with values lower than 0.5. For precipitation the observational uncertainty increases when synoptic patterns affecting the Mediterranean Basin are considered, reflecting the difficulty to properly capture the Mediterranean precipitation regimes.

### 1. Introduction

The Iberian Peninsula (IP), located in the southwest of Europe, between the midlatitude North Atlantic ocean and the Mediterranean sea, is characterized by a climate with large interannual and spatial variability (Cardoso et al., 2013; Esteban-Parra et al., 1998; Muñoz-Díaz & Rodrigo, 2004), significantly enhanced by coastal and/or land-ocean-atmosphere interaction processes, and complex topography (Knist et al., 2017; Rios-Entenza et al., 2014). This spatiotemporal climatic variability poses a challenge for (global and regional) climate models and, therefore, for the climate change impact analysis over the IP. Moreover, the IP is considered a climate change hot spot (Giorgi, 2006; Jerez et al., 2013; Viceto et al., 2017) due to projections of increasing temperatures, decreases in rainfall amounts, rising sea level, and intensifying extreme events, namely, droughts, heat waves, and extreme precipitation (Argeso et al., 2012; Cardoso et al., 2018; Soares et al., 2015, 2017; Turco et al., 2015).

Global climate models (GCMs) are the only modeling tool that enables the understanding of how the Earth system will evolve in response to the anthropogenic greenhouse gas emissions. However, the typical resolution of a GCM is still around 100 km, and, despite the notable ability of GCMs in representing the main properties of the large-scale atmospheric circulations (Meehl et al., 2007), they are unable to capture some of the physical processes (e.g., convection and clouds) that have a key role in defining the regional mean climate and extremes, especially at the subgrid scale (Frei et al., 2003; Randall et al., 2007; Soares, Cardoso, Miranda, de Medeiros, et al., 2012; Soares, Cardoso, Miranda, Viterbo, & Belo-Pereira, 2012). Downscaling techniques, both dynamical (Fernández et al., 2018) and statistical (Gutirrez et al., 2018), are used to fill this gap between the output of global models and the regional and local scales. In the case of the

dynamical approach, regional climate models (RCMs) use the output of the GCMs as boundary conditions to solve the atmospheric equations over a particular geographical domain (e.g., Europe), increasing the spatial and temporal resolutions and improving the modeling of the mesoscale processes (Laprise, 2008; Rummukainen, 2010).

The PRUDENCE (Christensen & Christensen, 2007) and ENSEMBLES (van der Linden & Mitchell, 2009) European projects were pioneer in promoting a coordinated regional climate modeling effort for climate change assessment studies in Europe, using horizontal resolutions of 50 and 25 km, respectively. In the last years, the World Climate Research Program, Coordinated Regional Downscaling Experiment (CORDEX) is coordinating a larger RCM ensemble for all continents (Giorgi et al., 2009). Due to the heterogeneity of the different CORDEX's domains both in number of simulations and GCMs and RCMs considered, making difficult to obtain a worldwide set of regional simulations, the multidomain CORDEX-CORE (Gutowski Jr et al., 2016) initiative was recently launched to provide a worldwide homogeneous foundation of high-resolution (0.22°) RCM simulations. To this aim the same core set of GCMs for the two scenarios RCP2.6 and RCP8.5 was considered.

In the context of EURO-CORDEX (Jacob et al., 2014), the European branch of CORDEX, the largest regional climate simulation effort was performed, which focused on a common European domain at two spatial resolutions 0.11° and 0.44°. The EURO-CORDEX set of runs included simulations of both evaluation, forced by ERA-Interim (Dee et al., 2011), and historical and future climate (Representative Concentration Pathway [RCP], Moss et al., 2010) experiments forced by global models. Despite the acknowledged model skills to reproduce the main temporal and spatial features of the European climate, it is also recognized that they are affected by nonnegligible bias (Katrakou et al., 2015; Kotlarski et al., 2014). Additionally, Kotlarski et al. (2017) investigated the influence of the observational uncertainty on the validation of the EURO-CORDEX evaluation experiment considering several European and national gridded observational data sets. The latter study showed that for most cases observational uncertainty is smaller than model uncertainty but for some subregions (e.g., Spain) and skill metrics (see figures 8 and 9 in Kotlarski et al., 2017) observational uncertainty may dominate. Hence, for those regions the selected observational reference data set may completely modify the RCM quality ranking.

In the IP, Casanueva et al. (2016) analyzed the evaluation experiment of EURO-CORDEX revealing significant model biases for seasonal precipitation in Spain, and a limited added value of the higher resolution when both 0.11° and 0.44° resolutions were compared mainly reflected on the rainfall spatial patterns. Soares et al. (2017) for precipitation and Cardoso et al. (2018) for temperatures compared the EURO-CORDEX historical results against observations, regular gridded and ground-based, respectively, showing that, although for precipitation there are a large spread and an overestimation of larger rainfall quantiles, the models can describe the temperatures and precipitation temporal and spatial patterns as well as its distributions. However, there are no a joint evaluation considering all the IP and a state-of-the-art high-resolution gridded data set.

Very recently, a new gridded data set including precipitation and temperatures (Herrera et al., 2019) was produced at 0.11° horizontal resolution (the rotated version), following previous efforts in which regular gridded data sets for Spain (Herrera, 2011; Herrera et al., 2012, 2015) and Portugal (Belo-Pereira et al., 2011, for precipitation only) were developed. This constitutes the first gridded data set for the IP including stations from both countries, with no border discontinuities and covering the period 1971–2015, allowing a proper evaluation of the EURO-CORDEX simulation on the IP.

In the current study, a set of simulations corresponding to the evaluation experiment of EURO-CORDEX is selected to evaluate the general models' behavior in reproducing the IP climate, from mean values to extremes. Only the higher resolution results are considered and directly compared with the new Iberia01 regular gridded data set. Furthermore, to illustrate the contribution of the observations and the RCMs to the uncertainty of models' evaluation, these are also compared with the E-OBS v19e gridded data set and the regional analysis EURO4M-MESAN. Finally, to further analyze the physical and/or geographical dependence of the observational uncertainty, the same analysis has been developed for precipitation but conditioned to an expert-knowledge-based weather typing method (Brands et al., 2014) and to the subregion of the IP, the Mediterranean or Atlantic Basins (see Figure 1).

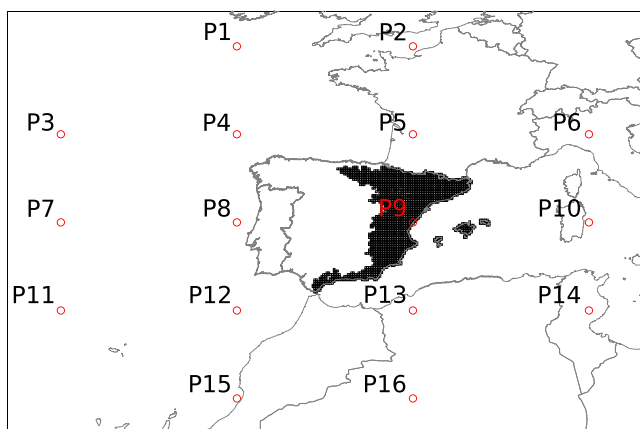


**Figure 1.** Coordinates considered for computing the Lamb weather types. The Iberian Peninsula has been divided in two subregions, the Mediterranean (black zone) and Atlantic (white zone) basins, for the observational uncertainty analysis.

one rotated at  $0.11^\circ$  and  $0.44^\circ$  spatial resolution, matching the grids considered in the EURO-CORDEX initiative, and another regular at  $0.10^\circ$  spatial resolution. For the evaluation of the RCMs we only consider the rotated version at  $0.11^\circ$ . On the other hand, in order to analyze the observational uncertainty in the evaluation of the RCMs, also the European gridded data set E-OBS v19e (Haylock et al., 2008), with a spatial resolution of  $0.10^\circ$ , was considered. This version includes the period 1950–2018 although this data set is periodically updated. E-OBS is the current reference gridded data set for daily precipitation and temperatures in Europe and has been previously used to analyze the observational uncertainty in the context of the evaluation of regional climate models (see, e.g., Kotlarski et al., 2017). Finally, the MESAN analysis developed in the framework of the European Reanalysis and Observations for Monitoring project (EURO4M) was considered. This data set includes several surface variables (e.g., precipitation and temperatures) covering the period 1989–2010 and has been downscaled at  $0.05^\circ$  resolution from a regional reanalysis of  $0.2^\circ$  spatial resolution, based on the high-resolution limited area model (HIRLAM), by means of optimal interpolation and the assimilation of surface observations.

## 2.2. EURO-CORDEX Regional Climate Models

Eight regional climate models from the European branch of the CORDEX initiative (EURO-CORDEX, Jacob et al., 2014) were considered in the present work (see Table 1) based on the maximization of the spread, so avoiding redundancies in the regional model selection, not only for the evaluation experiment but also for the climate change projections.

The *evaluation* experiment, in which the RCMs are driven by the reanalysis ERA-Interim (Dee et al., 2011), over the EUR-11 domain was considered to both evaluate the model quality in perfect conditions and have, at some point, day-to-day correspondence between the different data sets considered (observational gridded data sets, analysis, and RCMs) in order to be able to compare specific events occurred in particular dates.

**Table 1**  
ERA-Interim-Driven EURO-CORDEX (EUR-11) Simulations Considered

Model ID	Name_Version	Institution
RCM1	CLMcom-CCLM4-8-17_v1	Climate Limited-area Modelling Community
RCM2	SMHI-RCA4_v1	Swedish Meteorological and Hydrological Inst.
RCM3	KNMI-RACMO22E_v1	Royal Netherlands Meteorological Inst.
RCM4	DMI-HIRHAM5_v1	Danish Meteorological Inst.
RCM5	CNRM-ALADIN53_v1	Météo-France/C. National de Recherches Météorologiques
RCM6	DHMZ-RegCM4-2_v1	Meteorological and Hydrological Service of Croatia
RCM7	IPSL-INTERIS-WRF331F_v1	Inst. Pierre-Simon Laplace
RCM8	MPI-CSC-REMO2009_v1	Max Planck Inst.—Climate Service Center

The paper is structured as follows: First, in section 2 the observational data set, the models, and the evaluation methods used are summarized. Second, a detailed analysis of the EURO-CORDEX evaluation simulations performance is offered in section 3. Finally, the main conclusions and discussions grown from the analysis are detailed in section 4.

## 2. Data and Methods

### 2.1. Observations

Two observational gridded data sets and the analysis MESAN (Dahlgren & Gustafsson, 2012; Hggmark et al., 2000) have been considered in this study. On the one hand, Iberia01 (Herrera et al., 2019) is a new gridded observational data set of daily precipitation and temperatures for the Iberian Peninsula and the Balearic Island covering the period 1971–2015. This grid is based on a quality-controlled observational network of 3,487 and 276 stations for precipitation and temperature, respectively, belonging to the Spanish Agency of Meteorology (AEMET), the Portuguese Institute for Sea and Atmosphere (IPMA), and the Portuguese Environmental Agency (APA). Two versions of this data set have been developed,

**Table 2**  
*Precipitation and Temperature Indicators Used in This Study*

ID	Indicator	Units
pr	Mean daily precipitation amount	mm
RR1	Wet-day ( $pr > 1$ mm) frequency	%
RV50Yp	50-Year return value of daily precipitation	mm
tas	Mean daily 2-m air temperature	° C
RV50Yt	50-Year return value of the mean daily 2-m air temperature	° C

To keep the coherence between the different data sets, the period considered to make the analysis was imposed by the availability of the CORDEX's simulations, so we finally consider the period between 1989 and 2008 that is covered by all the data sets. Moreover, once the weather indices were estimated for each data set, observations, and RCMs, the resulting maps were interpolated to regular grid of  $0.1^\circ$  spatial resolution using the nearest neighbor approach.

Note that the eight RCMs considered are the basis of the EURO-CORDEX simulation with almost the 80% (19 over 25) of the simulations available in Earth System Grid Federation (ESGF archive, <https://esgf.org/>) for the EUR-11 domain for the historical and future experiments.

### 2.3. Weather Indicators

In order to analyze the mean and extreme regimes of precipitation and temperature the indicators reflected in Table 2 have been considered. In particular, to characterize the extreme regimes, the 50-year return value for each grid box was obtained by adjusting a generalized extreme value (GEV) distribution (Coles, 2001; Nikulin et al., 2011) to the series of annual maximum of daily values (for a detailed description see section 2.3 in Herrera et al., 2015). The GEV distribution is, by the extreme value theorem, the limit distribution of properly normalized maxima of a sequence of independent and identically distributed random variables, in our case the annual maximum of daily values, and it is characterized for three parameters: location ( $\mu$ ), scale ( $\psi$ ), and shape ( $\xi$ ) (see Equation 1).

$$GEV_{cdf}(x, \mu, \psi, \xi) = \begin{cases} \exp\left(-\exp\left(-\frac{x-\mu}{\psi}\right)\right), & \xi = 0; \\ \exp\left(-\left(1 - \xi \frac{x-\mu}{\psi}\right)^{\frac{-1}{\xi}}\right), & \xi \neq 0. \end{cases} \quad (1)$$

The shape parameter controls the behavior of the tail of the distribution, leading to three types of GEV distribution types: Gumbel ( $\xi = 0$ ) with a light, exponentially decaying tail; Fréchet ( $\xi > 0$ ) with a heavy, polynomial-decaying tail; and Weibull ( $\xi < 0$ ) with a short, bounded tail. The optimal model parameters are estimated by maximizing the log-likelihood function (Mínguez et al., 2013). For the sake of parsimony, when the 95% confidence interval of the shape parameter ( $\xi$ ) contains the value 0, then the shape parameter is fixed to 0 ( $\xi = 0$ ), and the other two parameters of the distribution (location and scale) are re-estimated.

In the case of precipitation, due to the dual nature of this variable (binary and continuous), also the frequency of wet days has been considered for the characterization of the mean regime.

### 2.4. Validation Measures

For each observational data set, grid box, model, variable, and season (annual, winter, spring, summer, and autumn) the following validation measures were considered:

$$BIAS_{rcm} = \bar{Y}_{rcm} - \overline{obs}, \quad (2)$$

$$BIAS_{rcm}^{rv50} = RV50(Y_{rcm}) - RV50(obs), \quad (3)$$

$$RATIO_{rcm} = STD(Y_{rcm}) / STD(obs), \quad (4)$$

$$BIASrel_{rcm} = 100 * (\bar{Y}_{rcm} - \overline{obs}) / \overline{obs}, \quad (5)$$

$$RATIO_{rcm}^{rr1} = WDFR(Y_{rcm})/WDFR(obs), \quad (6)$$

where the  $\bar{X}$  corresponds to the mean of the variable  $X$  (e.g.,  $obs$ ),  $STD$  refers to the standard deviation,  $RV50$  refers to the 50-year return value, and  $WDFR$  refers to the wet-day frequency. The latest two equations should be considered in the case of precipitation, for which the relative bias is obtained for both the mean and the 50-year return value.

For the sake of the comparability and coherence with the work of Kotlarski et al. (2017) also the performance metrics defined in this paper were considered:

$$BIAS_{rcm} = \overline{\langle \bar{Y}_{rcm} - \bar{obs} \rangle}, \quad (7)$$

$$BIAS_{rcm}^{rv50} = \overline{\langle RV50(Y_{rcm}) - RV50(obs) \rangle}, \quad (8)$$

$$MAE99_{rcm} = \overline{\langle |P99(Y_{rcm}) - P99(obs)| \rangle}, \quad (9)$$

$$MAE01_{rcm} = \overline{\langle |P01(Y_{rcm}) - P01(obs)| \rangle}, \quad (10)$$

$$PACO_{rcm} = \frac{COV(\bar{Y}_{rcm}, \bar{obs})}{STD(\bar{Y}_{rcm})STD(\bar{obs})}, \quad (11)$$

$$RIAV_{rcm} = \frac{STD(\bar{Y}_{rcm})}{\overline{\overline{STD}}(obs)}, \quad (12)$$

$$WDFREQ_{rcm} = \overline{\langle |WDFR(Y_{rcm}) - WDFR(obs)| \rangle}, \quad (13)$$

where  $COV$  and  $P01$  and  $P99$  are the spatial covariance and the 1st and 99th percentiles, respectively. Note that the two-sample Kolmogorov-Smirnov test (K-S test, Lopes, 2011) is applied to the standardized (centered and normalized) series in order to isolate differences in the distribution of both time series not reflected by the rest of validation measures, in particular the  $BIAS$  and the  $RATIO$ .

Finally, two hypothesis tests, the  $t$  test and the  $F$  test, have been considered to assess if the mean and variance of the different data set are or not equal at some significant level. As a result, for each grid point and hypothesis test the  $p$  value and the rejection (or not) of the null hypothesis were obtained. For the wet-day frequency the two-sample Z test for proportions was considered, and the interval confidence of the 50-year return value obtained after the adjustment of the GEV distribution was used to estimate the statistical significance at which the 50-year return values of two data sets are different. To this aim, for each grid box the confidence intervals at 85% level of significance of the 50-year return values of two data sets were obtained. If there is not overlapping between both intervals, we could conclude that the return values are different at the 95% level of confidence. If there is no overlapping, we could conclude that the return values are different at the 95% level of confidence (Goldstein & Healy, 1995; Julius, 2004).

## 2.5. Uncertainty Intercomparison

Kotlarski et al. (2017) defined a framework to quantify the relation between the uncertainty of the evaluation results due to the observational data set considered as reference and to the RCMs. The availability of several reference data sets lets us to apply, in this paper, the same analysis at a seasonal and annual scales considering three observational data sets ( $i \in \{1, 2, 3\}$ ) (Iberia01, E-OBS v19e, and EURO4M MESAN) and eight RCMs ( $j \in \{1, \dots, 8\}$ ), obtaining the following expressions for each validation measure  $M$ :

$$U_{obs} = \frac{1}{8} \sum_{j=1:8} \sqrt{\frac{1}{2} \sum_{i=1:3} \left( M_{i,j} - \frac{1}{3} \sum_{i=1:3} M_{i,j} \right)^2}, \quad (14)$$

$$U_{rcm} = \frac{1}{3} \sum_{i=1:3} \left( \frac{1}{56} \sum_{n=1:56} \sqrt{\frac{1}{2} \sum_{j \in S_n} \left( M_{i,j} - \frac{1}{3} \sum_{i=1:3} M_{i,j} \right)^2} \right), \quad (15)$$

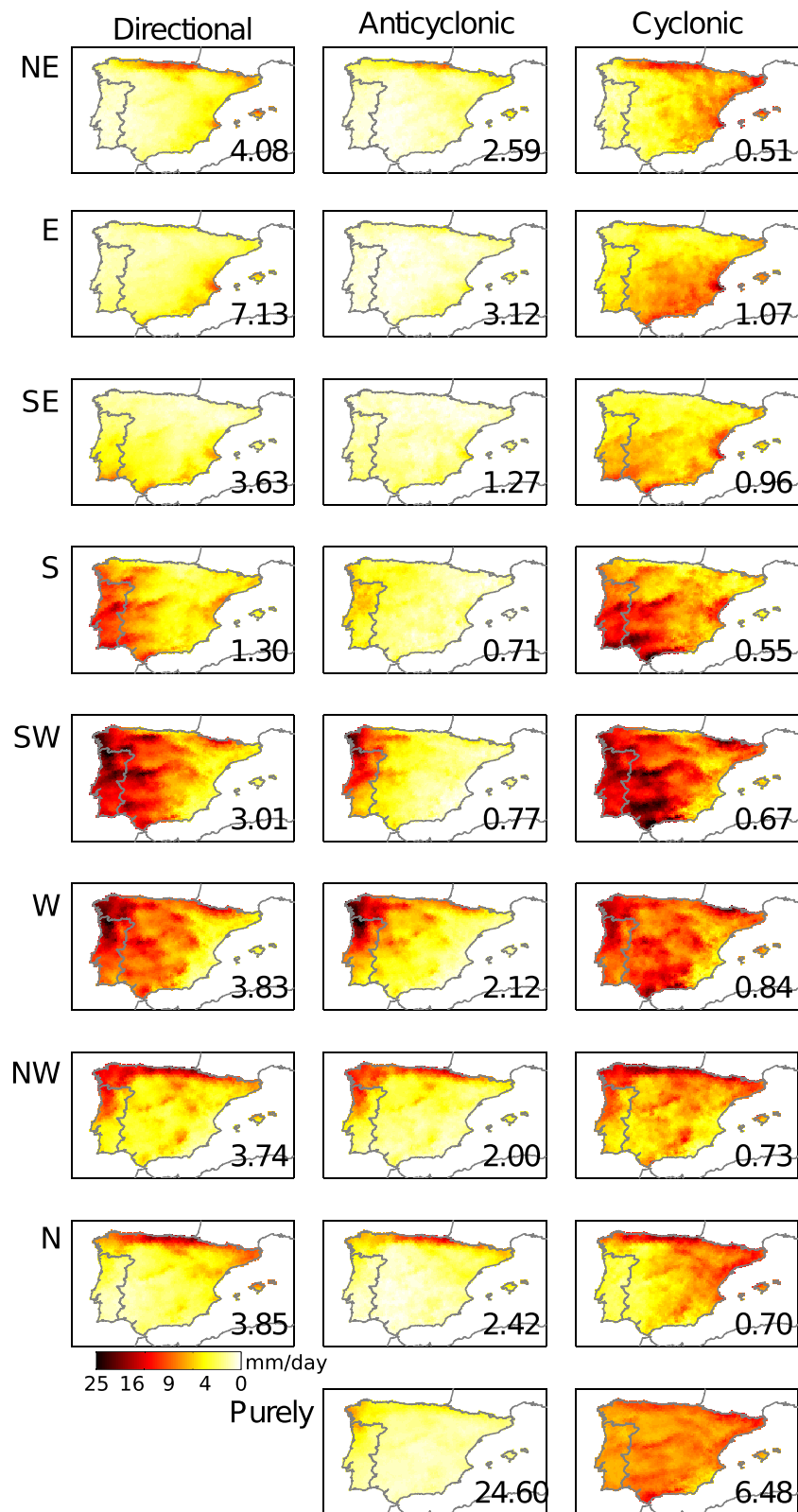


**Figure 2.** Mean daily precipitation, as given by Iberia01, of the 26 original Lamb weather types for the period 1989–2008. The numbers correspond to the frequency of each WT.

**Table 3**  
*Percentage of Statistically Significant—at 95 % Level—Different Grid Boxes of E-OBS v19e, MESAN, and the Eight RCMs Considering Iberia01 as Reference*

Data Set	Temp.			Precip.			
	Mean	STD	RV50	Mean	STD	RV50	WDFR
E-OBS v19e	80.22	63.54	78.95	82.80	98.00	95.25	90.93
MESAN	81.67	65.12	75.04	63.33	88.59	89.33	94.73
RCM1	79.77	98.43	60.68	79.79	89.67	87.83	100.0
RCM2	93.75	88.83	55.26	76.14	93.30	91.62	85.06
RCM3	94.44	95.44	65.16	62.35	92.87	88.98	78.33
RCM4	81.53	91.20	74.56	82.84	92.58	86.85	99.64
RCM5	88.83	98.66	76.74	82.51	93.96	89.60	88.43
RCM6	91.98	90.00	24.84	91.48	93.58	88.24	93.34
RCM7	83.30	73.51	84.13	75.88	92.51	87.21	99.98
RCM8	86.90	90.72	51.13	77.74	92.31	85.85	99.88

$$U_{ratio} = \frac{U_{obs}}{U_{rcm}}, \quad (16)$$

where  $S_n$  are all the possible combinations without replicas of the eight models available (56). The first equation quantifies the observational uncertainty of a given measure ( $M$ ) as the mean between RCMs of the standard deviations of the measure obtained comparing an RCM against each observational reference. The second equation quantifies the model uncertainty considering the mean of the standard deviations obtained for each combination of three RCMs, to be coherent with  $U_{obs}$ , without replicas when compared with each a given observational reference. Finally, for a given measure, variable, and season, the  $U_{ratio}$  defines the relation between both uncertainties, with values greater than 1 reflecting that the observational data set introduces more uncertainty to the evaluation than the models and vice versa.

## 2.6. Lamb Weather Types

As has been previously reflected, the location of the IP and the effect of the Mediterranean Sea and the Atlantic Ocean lead to a large spatial climatic variability. In particular, a strong northwest-southeast gradient is observed for precipitation, with characteristic Atlantic and Mediterranean regimes. Moreover, Kotlarski et al. (2017) pointed out that, for some regions, including Spain, and skill metrics the observational component could dominate the uncertainty in the models' evaluation. To further analyze this point and identify the synoptic patterns affecting each region, the expert-knowledge-based Lamb weather typing centered over the IP was considered (Brands et al., 2014), obtaining the 26 weather types shown in Figure 2 and a 27th class including the nonclassified cases. This clustering approach is based on daily sea-level pressure, obtained from the reanalysis ERA-Interim (Dee et al., 2011), over the points shown in Figure 1, and is defined by a rule-based classification algorithm in which the types are predefined based on meteorological expert knowledge (Lamb, 1972; Trigo & DaCamara, 2000).

## 3. Results

Table 3 shows the differences found for precipitation and temperature between Iberia01 and both the reference data sets and the RCMs, based on the hypothesis tests previously described. Regarding the reference data sets, the results for temperature are more homogeneous than for precipitation, in which the analysis MESAN outperforms E-OBS v19e for all the parameters excepting the wet-days frequency. In any case, at least the 63% of the grid boxes present significant differences with Iberia01 for all the parameters and data sets, reflecting a high observational uncertainty. Regarding the RCMs, almost all the differences are greater than 60%, being the STD parameter the one reaching the largest differences for all the RCMs and variables (Temp.: 73.51–98.66; Precip.: 89.67–93.96). As a difference with the observational references, there is a great heterogeneity between the RCMs in the case of the 50-year return value of temperature with differences ranging between 24.84% and 84.13% while in the case of precipitation the behavior is more homogeneous with all the values greater than 85.85%.

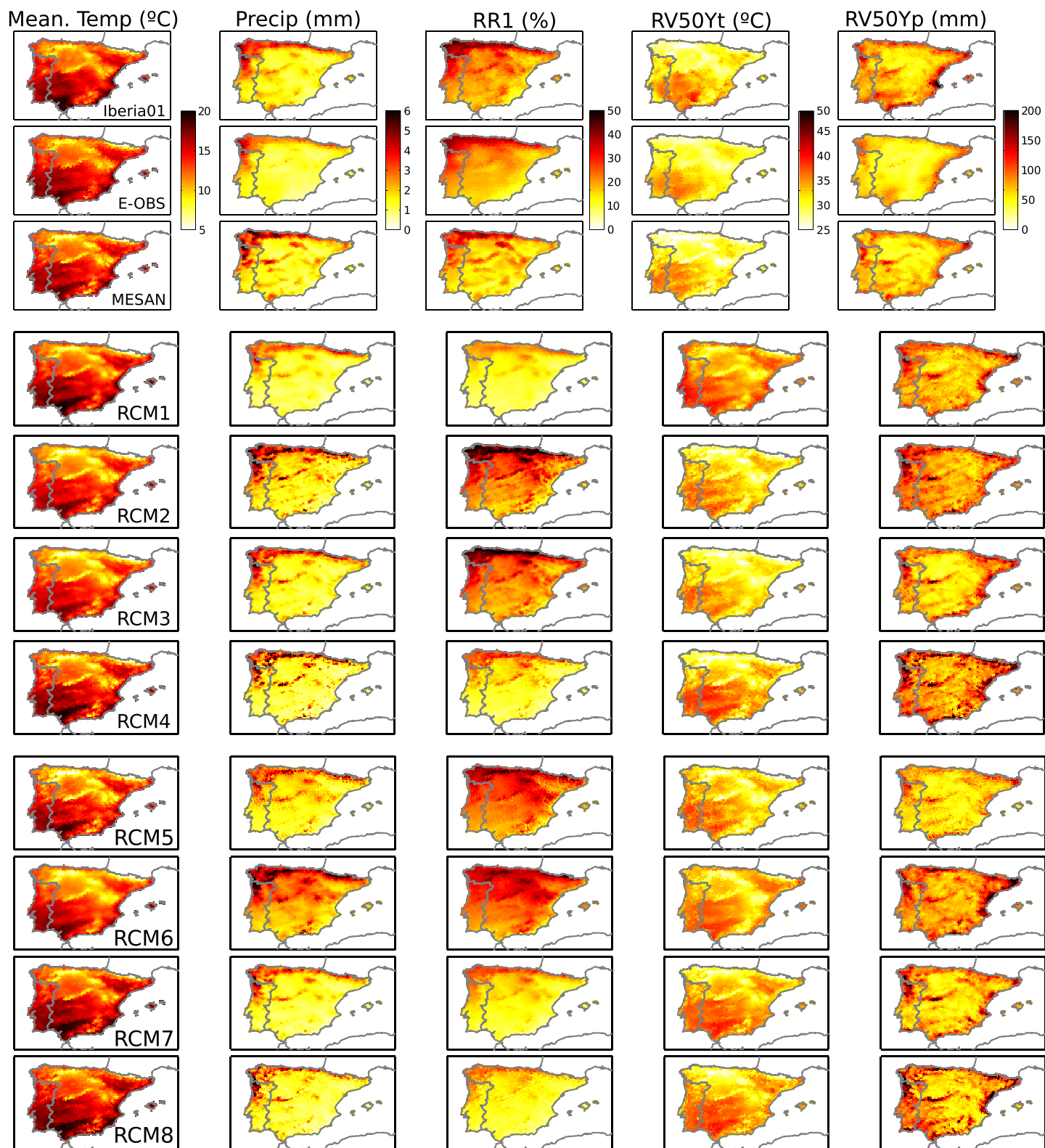
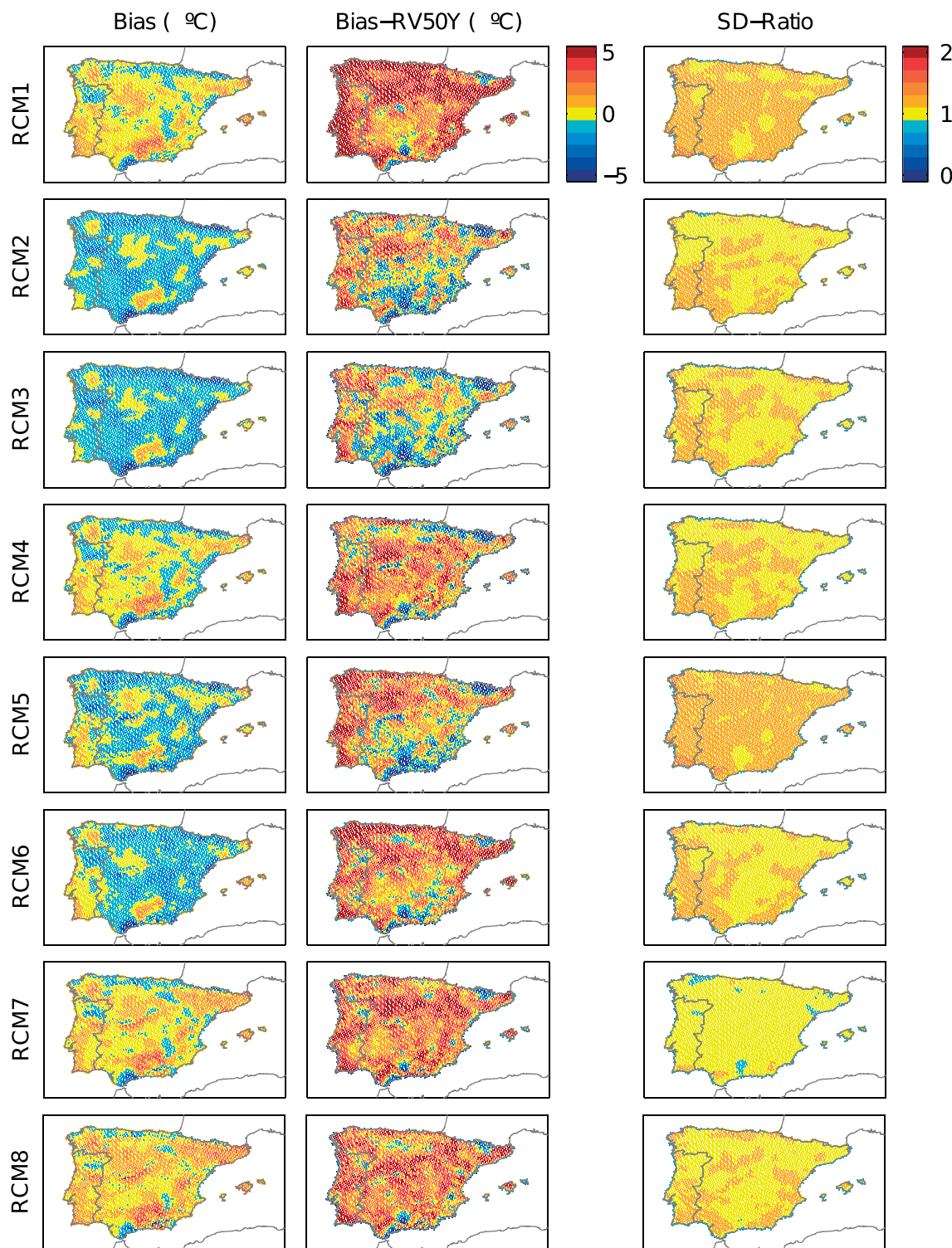
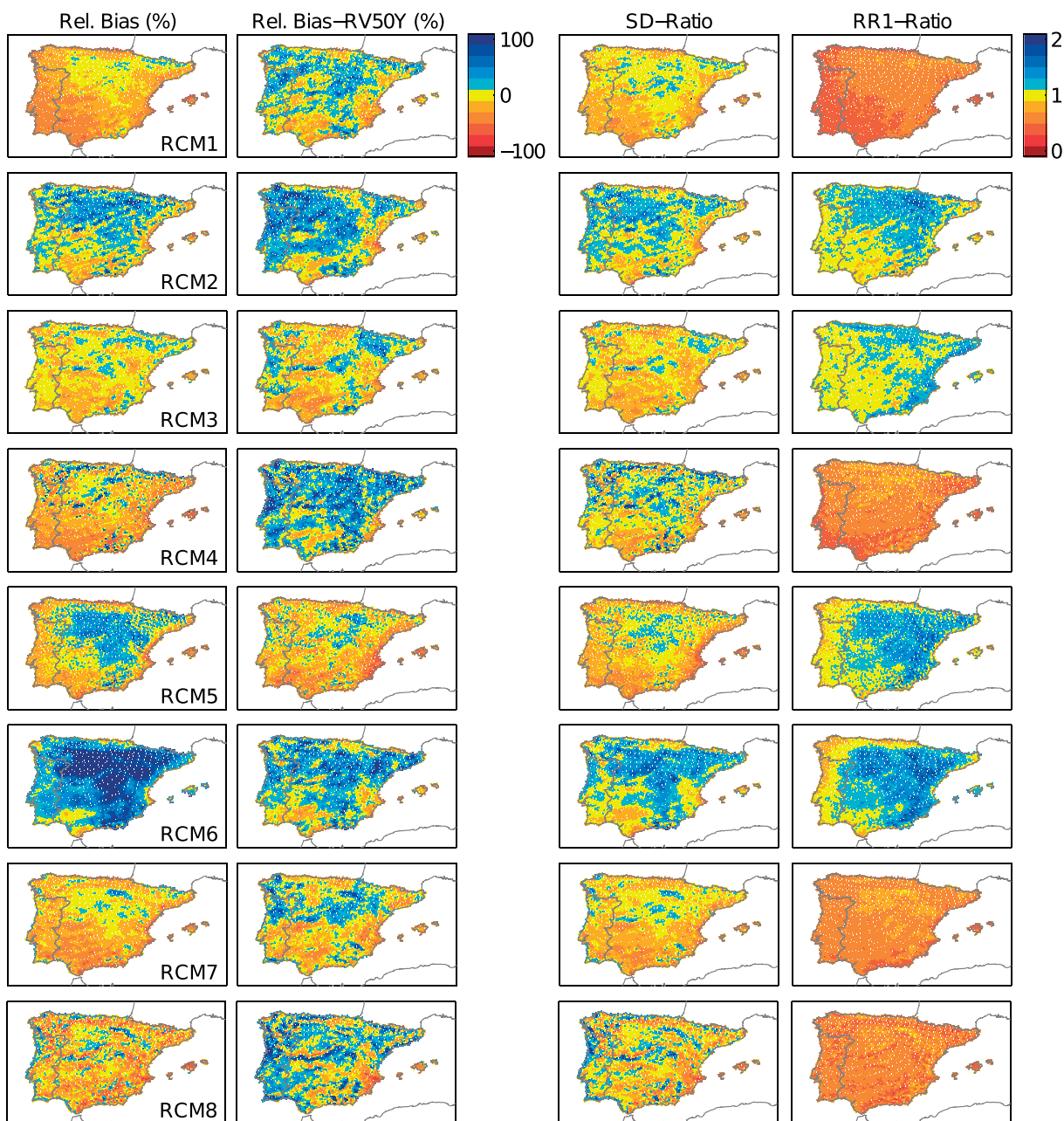


Figure 3. Climatology of the period 1989–2008 for the weather indices of precipitation and temperature defined in Table 2.



**Figure 4.** Bias with respect to Iberia01 of the mean temperature (first column) and the 50-year return value (second column) of daily mean temperature and ratio between the simulated and observed standard deviation (third column) of the eight models defined in Table 1.



**Figure 5.** Relative bias with respect to Iberia01 of the precipitation (first column) and the 50-year return value (second column) of the maximum daily precipitation, ratios between the simulated and observed standard deviation (third column), and wet-day frequency (fourth column) of the eight models defined in Table 1.

### 3.1. Weather Indicators

Figure 3 shows the climatology for the period 1989–2008 of the indices defined in Table 2 (in columns) for Iberia01, E-OBS v19e, MESAN, and the eight RCMs (in rows). A spatial view of the differences between models and Iberia01 is depicted in Figures 4 and 5 for temperature and precipitation, respectively. Note that the behavior of the RCMs strongly depends on the variable considered, with more coherence between data sets for temperature than for precipitation. However, within the precipitation-based indices, there is no a clear division among RCMs due to the different performances between indices. For example, RCM3 and RCM7 have a different pattern for RR1 but very similar for RV50Yp and pr. Table 4 summarizes the results for the validation measures proposed in section 2.

**Table 4**  
*Validation Measures for Each Regional Climate Model*

Validation measure	RCM1	RCM2	RCM3	RCM4	RCM5	RCM6	RCM7	RCM8
Temperature								
PACO	0.95	0.94	0.94	0.94	0.92	0.93	0.93	0.92
MAE99	3.30	1.13	1.11	1.83	1.72	1.59	1.58	2.11
MAE01	1.27	1.73	2.40	1.23	2.18	1.25	1.36	1.33
BIAS <sup>a</sup>	0.13	-1.12	-1.20	-0.12	-0.81	-0.88	0.31	0.70
BIAS <sup>r50 a</sup>	3.44	0.45	-0.19	1.22	1.08	2.01	2.00	1.89
RATIO <sup>a</sup>	1.14	1.08	1.08	1.07	1.16	1.06	0.98	1.06
Precipitation								
PACO	0.88	0.87	0.92	0.77	0.78	0.80	0.90	0.78
MAE99	4.07	4.76	4.27	6.49	5.69	5.35	4.86	6.52
BIASrel <sup>a</sup>	-21.13	11.41	-5.07	-13.35	1.25	53.71	-15.81	-13.93
BIASrel <sup>r50 a</sup>	6.93	19.34	-2.62	26.07	-13.35	20.38	0.14	16.55
RATIO <sup>a</sup>	0.91	1.08	0.90	1.03	0.87	1.16	0.88	0.97
RATIO <sup>r1 a</sup>	0.53	1.12	1.10	0.59	1.14	1.20	0.63	0.59

<sup>a</sup> Measures that correspond to the spatial mean.

Regarding temperature indices, the eight RCMs reproduce properly the standard deviation (*RATIO*), with a mean overestimation of 7% approximately and the spatial pattern of the mean values (*PACO*) showing similar underestimation values. In the case of extreme values, the RCMs tend to overestimate the 50-year return value around 1°C with the greatest bias shown by the RCM1 (more than 3°C) and the lowest by the RCM3 (less than -0.1°C). The overestimation obtained for the return value by the RCM1 is also reflected to the *MAE99* with the rest of the models having values ranging between 1°C and 2°C, approximately. In spite of the spatial mean values shown in Table 4 for the *BIAS<sup>r50 a</sup>*, the results shown in Figure 4, combined with the values of *MAE01* and *MAE99* of Table 4, that reflect than the lowest values for both biases, *BIAS* and *BIAS<sup>r50 a</sup>*, are due to the compensation effect of the spatial average.

A greater dependence on the index considered is found in the case of precipitation. For the mean regime, given by the *BIAS* and *RATIO<sup>r1 a</sup>*, the eight RCMs could be divided in two groups. On the one hand, RCM1, RCM4, RCM7, and RCM8 show a general underestimation of both parameters with only isolated points with some overestimation (see Figure 5). On the other hand, RCM2, RCM3, RCM5, and RCM6 reflect spatial patterns combining regions with positive bias and areas without bias or close to 0. Finally, the groups identified for the mean regime are not preserved for the other two indices in which there is no general behavior of the eight RCMs. This heterogeneity is also reflected by the validation measures shown in Table 4. In general, the performance for precipitation is clearly worst than for temperature, being the spatial pattern (*PACO*) and the standard deviation (*RATIO*) the only indices with values comparable at some point.

In Figure 4 it can be seen that most of the RCMs reveal some tendency to overestimate mean temperature over the major river valleys (e.g., Guadalquivir and Douro). Regarding the temperature 50-year return values, the majority of RCMs consistently show an underestimation over the Pyrenees. This is also true in a small region west of Sierra Nevada but may due to a rather low ground-based observations density.

Based on the results shown in Table 4, we can obtain the ranking for each RCM and observational reference (Figure 6) following the approach proposed in Kotlarski et al. (2017). First, there are RCMs for which the rank strongly depends on the observational reference and/or variable (e.g., RCM2, RCM4, or RCM5). According to Figure 6, the RCM1, RCM3, RCM6, RCM7, and RCM8 are the ones with less variability although only RCM3 and RCM7 have a good ranking among the eight RCMs.

### 3.2. Uncertainty Intercomparison

Table 5 shows the results obtained in the uncertainty analysis for all the seasons and validation measures defined in section 2.4 and used in the work of Kotlarski et al. (2017). In this case, we have extended the analysis to the minimum and maximum temperatures, which have not been included in the previous analysis for the sake of the brevity.

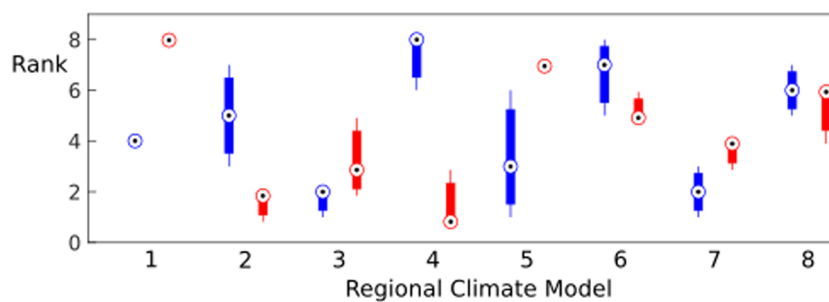


**Figure 6.** Ranking of the eight models defined in Table 1 according to the equations defined by Kotlarski et al. (2017) and described in section 2.4. Blue boxes correspond to precipitation, and red boxes correspond to mean temperature.

As has been reflected in previous sections, we have different conclusions for precipitation and temperatures. For the former, both the observational and the model uncertainties are, at least, comparable for almost all the indices and seasons. Only the wet-day frequency (last column) and some isolated cases (e.g., PACO index in summer) show a clear significant contribution to the uncertainty of the model with reference to the observations. In agreement with the results shown in Figure 5 the index with the largest observational uncertainty for precipitation is the bias corresponding to the 50-year return value (third column).

Regarding the mean temperature, the weight of the model increases in comparison with the results obtained for precipitation with most of the values lower than 0.5, reflecting that the model uncertainty doubles the observational uncertainty. In contrast with precipitation, in this case only the spatial pattern PACO and some isolated cases show values close to 1. These results are in agreement with the found by Herrera et al. (2019) in which both observational data sets were found statistically equivalent in the sense that their differences

**Table 5**  
*Ratio Between the Observational and the RCM Uncertainties for Each Season (Rows) and Validation Measure (Column),  $U_{ratio}$*

Precipitation	BIAS	MAE99	BIAS <sup>r50</sup>	PACO	K – S	RIAV	WDFREQ
Annual	0.88	1.09	2.03	0.77	1.00	1.66	0.03
Winter	0.89	1.01	2.35	0.84	1.00	1.40	0.04
Spring	0.66	1.43	2.16	0.74	1.00	0.69	0.22
Summer	0.43	0.89	2.94	0.23	1.01	0.49	0.31
Autumn	1.00	1.09	2.02	0.92	1.00	1.28	0.03
Mean Temp.	BIAS	MAE99	BIAS <sup>r50</sup>	PACO	K – S	RIAV	MAE01
Annual	0.09	0.18	0.67	0.96	1.00	0.67	0.14
Winter	0.01	0.13	0.11	0.82	0.59	0.15	0.18
Spring	0.13	0.29	0.26	0.89	0.38	0.58	0.27
Summer	0.18	0.22	0.70	0.78	1.08	0.36	0.45
Autumn	0.04	0.27	0.48	0.89	0.50	0.07	0.11
Max Temp.	BIAS	MAE99	BIAS <sup>r50</sup>	PACO	K – S	RIAV	MAE01
Annual	0.32	0.55	0.80	0.95	1.00	0.54	0.34
Winter	0.20	0.62	0.46	1.80	0.90	0.39	0.41
Spring	0.29	0.95	0.21	0.78	0.94	0.23	0.13
Summer	0.30	0.51	0.80	0.43	0.37	0.35	0.24
Autumn	0.23	0.64	0.72	1.19	0.92	0.19	0.19
Min Temp.	BIAS	MAE99	BIAS <sup>r50</sup>	PACO	K – S	RIAV	MAE01
Annual	0.16	0.08	0.15	1.09	1.00	0.78	0.50
Winter	0.16	0.61	0.18	0.93	1.08	0.09	0.45
Spring	0.09	0.13	0.12	0.87	1.32	0.99	0.36
Summer	0.15	0.10	0.05	1.56	0.33	0.32	0.36
Autumn	0.20	0.15	0.33	1.05	0.72	0.09	0.61

**Table 6**

The  $U_{ratio}$  Over the IP, the Atlantic Basin, and the Mediterranean Basin, Respectively, and the Impact of Each WT, as Given by the Ratio Between the Percentage of the Total Precipitation due to the Weather Type and its Frequency

Iberian Peninsula	NE	E	SE	S	SW	W	NW	N	Purely
Directional	0.72	0.65	0.61	0.75	0.80	0.75	0.49	0.92	
Anticyclonic	0.37	0.20	0.28	0.32	0.54	0.61	0.44	0.48	0.29
Cyclonic	0.88	0.89	0.79	1.00	0.94	0.87	1.18	0.90	1.60
Mediterranean	NE	E	SE	S	SW	W	NW	N	Purely
Directional	0.53	0.48	0.55	1.89	3.77	2.94	1.41	0.94	
Anticyclonic	0.20	0.09	0.15	0.38	1.03	1.46	0.73	0.36	0.22
Cyclonic	1.44	1.91	1.54	3.31	5.19	3.76	2.21	1.96	2.78
Atlantic	NE	E	SE	S	SW	W	NW	N	Purely
Directional	0.25	0.24	0.53	2.21	4.84	3.66	1.45	0.64	
Anticyclonic	0.11	0.04	0.13	0.49	1.42	1.93	0.80	0.25	0.23
Cyclonic	0.83	1.52	1.39	3.67	6.03	4.04	2.13	1.31	2.54
WT impact	NE	E	SE	S	SW	W	NW	N	Purely
Directional	1.08	0.96	0.59	1.25	1.62	1.50	1.32	1.54	
Anticyclonic	0.38	0.20	0.21	0.16	0.23	0.51	0.59	0.58	0.18
Cyclonic	2.67	2.69	1.83	2.58	3.50	3.22	2.38	3.27	3.26

could be assimilated as noise. Finally, as could be expected for the maximum and minimum temperatures, the results are similar to the obtained for the mean, with the main differences reached for the extremes MAE99 and MAE01 for maximum and minimum temperatures, respectively, as they represent the upper and lower tails of the distribution.

Considering the same analysis for precipitation (the same has been done for temperature, but the results and conclusions are the same as the obtained for the full series) and each weather type and subregion (see subsection 2.6), we found a dependence between the weight of the observational reference and the impact of each weather type, as given by the ratio between the percentage of the total precipitation due to the weather type and his frequency, with Pearson's correlation coefficient of 0.84 for the Mediterranean Basin, 0.54 for the Atlantic Basin, and 0.66 for all the IP. Table 6 shows the results for the impact parameters. As can be seen in the table, the impact and weight of the observational component over the Mediterranean increase from the anticyclonic types to the cyclonic types. For the Atlantic Basin, although the impact also increases in a similar way, the observations have, more or less, the same relevance for the directional and cyclonic types. This result illustrates the difficulty of the observational data set to properly reproduce the Mediterranean precipitation regimes, leading to a greater uncertainty of this component.

#### 4. Conclusions and Discussion

In this work the recently developed Iberia01 data set has been used to evaluate a representative ensemble containing eight reanalysis-driven regional climate models, representing the basis of the EURO-CORDEX simulations for the historical and future experiments of the EUR-11 domain available in ESGF. To this aim, several weather indices reflecting the mean and extreme regimes of precipitation and mean temperature have been obtained for the observational data set and the models and compared by means of different validation measures. In addition, the European grid E-OBS v19e was considered in order to quantify the contribution of the observational uncertainty to the variability of the results obtained in the evaluation of the models following the framework proposed by Kotlarski et al. (2017).

On the one hand, the models show a great coherence for temperature, being able to reproduce properly the observed spatial pattern and variability. The main problems appear for the extremes (50-year return value) for which a general overestimation has been found, reaching in some cases up to 3° C. In contrast, in the case of precipitation the performance of the models depends on the weather index considered, with only the DHMZ-RegCM4-2.v1 (RCM6 in Table 1) showing a general overestimation of all the parameters. Although the models are, more or less, able to reproduce the spatial pattern (PACO) and the variability (RATIO)

of the precipitation, a strong bias is obtained for both the mean precipitation and the 50-year return value that can reach until the 25% and the 50% of the observed values, respectively.

On the other hand, in the case of the observational uncertainty analysis, also the maximum and minimum daily temperatures were considered in order to obtain a more general picture of this topic. As could be expected, a higher dependence on the observational data set has been found for precipitation than for temperature. This uncertainty is particularly significant when the 50-year return value is considered for which the observational uncertainty doubles the model uncertainty. Only the wet-day frequency presents values lower than 0.5 for all the seasons, with the rest of values, with isolated exceptions, reflecting a similar contribution of both components, model and observations, to the uncertainty. In the case of temperatures, the main contribution of the observations has been found when the lower (MAE01) and upper (MAE99) extremes are considered with most of the values lower than 0.5. Note that the complex orography and the influence of both the Atlantic Ocean and the Mediterranean Sea modulate the precipitation over the Iberian Peninsula, leading to particular regimes, as the cold drops in the east coast, that a continental adjustment of the interpolation model is not able to reproduce, even more when a low-dense observational network is considered. In this sense, the large increase of rain gauges considered in Iberia01, when compared with E-OBS v19e, gives rise to a much improved precipitation rendering. In the case of temperature, although the observational network considered is similar in both cases, the pattern tends to be more orographic in E-OBS v19e due to the continental adjustment of the interpolation method that overrates this component avoiding regional behaviors. In addition, the contribution of the observational network considered in France also has a clear effect on the interpolated value over the Pyrenees and the northeast of the Iberian Peninsula.

Based on the previously described results, we have obtained the ranking for each RCM and observational reference, being the RCM3 (KNMI-RACMO22E v1) and RCM7 (IPSL-INTERIS-WRF331F v1) the ones with less variability among variables and observational reference and with a good enough ranking among the eight RCMs.

Finally, in order to identify the synoptic patterns related with a higher contribution to the observational uncertainty the Lamb weather-type classification based on the sea-level pressure over the Iberian Peninsula was considered. The observational uncertainty analysis conditioned to the obtained weather types reflects the difficulty of the observational data set to properly reproduce the Mediterranean precipitation regimes, leading to a greater observational uncertainty over this region that increases from the anticyclonic types to the cyclonic types. For the Atlantic Basin the observations have the same relevance for the directional and cyclonic types.

## Data Availability Statement

All the data sets used in this work are publicly available. The Iberia01 data set (<https://doi.org/10.20350/digitalCSIC/8641> Gutiérrez et al., 2019) is publicly available through the Digital CSIC Open Science portal: <https://hdl.handle.net/10261/183071>. The E-OBS v19e data set is available through the Copernicus Climate Change Service (C3S): [https://surfobs.climate.copernicus.eu/dataaccess/access\\_eobs.php](https://surfobs.climate.copernicus.eu/dataaccess/access_eobs.php).

## References

- Argeso, D., Hidalgo-Muoz, J., Gmiz-Fortis, S., Esteban-Parra, M., & Castro-Dez, Y. (2012). High-resolution projections of mean and extreme precipitation over Spain using the WRF model (20702099 versus 19701999). *Journal of Geophysical Research*, 117, D12108. <https://doi.org/10.1029/2011JD017399>
- Belo-Pereira, M., Dutra, E., & Viterbo, P. (2011). Evaluation of global precipitation data sets over the Iberian Peninsula. *Journal of Geophysical Research*, 116, D20101. <https://doi.org/10.1029/2010JD015481>
- Brands, S., Herrera, S., & Gutirrez, J. M. (2014). Is Eurasian snow cover in October a reliable statistical predictor for the wintertime climate on the Iberian Peninsula? *International Journal of Climatology*, 34(5), 1615–1627. <https://doi.org/10.1002/joc.3788>
- Cardoso, R., Soares, P., Lima, D., & Miranda, P. (2018). Mean and extreme temperatures in a warming climate: EURO CORDEX and WRF regional climate high-resolution projections for Portugal. *Climate Dynamics*, 52, 129–157. <https://doi.org/10.1007/s00382-018-4124-4>
- Cardoso, R., Soares, P., Miranda, P., & Belo-Pereira, M. (2013). WRF high resolution simulation of Iberian mean and extreme precipitation climate. *International Journal of Climatology*, 33(11), 2591–2608. <https://doi.org/10.1002/joc.3616>
- Casanueva, A., Kotlarski, S., Herrera, S., Fernández, J., Gutiérrez, J. M., Boberg, F., et al. (2016). Daily precipitation statistics in a EURO-CORDEX RCM ensemble: Added value of raw and bias-corrected high-resolution simulations. *Climate Dynamics*, 47(3), 719–737. <https://doi.org/10.1007/s00382-015-2865-x>
- Christensen, J., & Christensen, O. (2007). A summary of the PRUDENCE model projections of changes in European climate by the end of this century. *Climatic Change*, 81(1), 7–30. <https://doi.org/10.1007/s10584-006-9210-7>
- Coles, S. (2001). *An introduction to statistical modeling of extreme value*. Berlin and Heidelberg: Springer-Verlag.

## Acknowledgments

This work was partially funded by the Spanish Government R&D Programme (Exp. CGL2010-21869 and CGL2010-22158-C02) and the European Comission (INDECIS: H2020-690462). Pedro M. M. Soares and Rita M. Cardoso wish to acknowledge the SOLAR (PTDC/GEOMET/7078/2014) project and the funding by the Instituto Dom Luiz (Project FCT UID/GEO/50019/2019).

The authors are grateful to the Portuguese Institute for Sea and Atmosphere (IPMA) and the Portuguese Environmental Agency for providing the needed observational data. The authors are also grateful to AEMET for providing the necessary data to do this work. We acknowledge the E-OBS data set from the EU-FP6 project ENSEMBLES (<http://ensembles-eu.metoffice.com>) and the data providers in the ECA&D project (<http://www.ecad.eu>). We acknowledge the E-OBS data set from the EU-FP6 project UERRA (<http://www.uerra.eu>) and the Copernicus Climate Change Service and the data providers in the ECA&D project (<https://www.ecad.eu>).

We thank the editor and anonymous reviewers participating in the different versions of this paper for their constructive comments, which have significantly contributed to improve this article.

- Dahlgren, P., & Gustafsson, N. (2012). Assimilating host model information into a limited area model. *Tellus A: Dynamic Meteorology and Oceanography*, 64(1), 15836. <https://doi.org/10.3402/tellusa.v64i0.15836>
- Dee, D. P., Uppala, S., Simmons, A., Berrisford, P., Poli, P., Kobayashi, S., et al. (2011). The ERA-Interim reanalysis: Configuration and performance of the data assimilation system. *Quarterly Journal of the Royal Meteorological Society*, 137, 553–597. <https://doi.org/10.1002/qj.828>
- Esteban-Parra, M., Rodrigo, F., & Castro-Diez, Y. (1998). Spatial and temporal patterns of precipitation in Spain for the period 1880–1992. *International Journal of Climatology*, 18(14), 1557–1574. [https://doi.org/10.1002/\(SICI\)1097-0088\(19981130\)18:14<1557::AID-JOC328>3.0.CO;2-J](https://doi.org/10.1002/(SICI)1097-0088(19981130)18:14<1557::AID-JOC328>3.0.CO;2-J)
- Fernández, J., Frías, M. D., Cabos, W. D., Cofiño, A. S., Dominguez, M., Fita, L., et al. (2018). Consistency of climate change projections from multiple global and regional model intercomparison projects. *Climate Dynamics*, 52, 1139–1156. <https://doi.org/10.1007/s00382-018-4181-8>
- Frei, C., Christensen, J. H., Déqué, M., Jacob, D., Jones, R. G., & Vidale, P. L. (2003). Daily precipitation statistics in regional climate models: Evaluation and intercomparison for the European alps. *Journal of Geophysical Research*, 108(D3), 4124. <https://doi.org/10.1029/2002JD002287>
- Giorgi, F. (2006). Climate change hot-spots. *Geophysical Research Letters*, 33, L08707. <https://doi.org/10.1029/2006GL025734>
- Giorgi, F., Jones, C., & Asrar, G. R. (2009). Addressing climate information needs at the regional level: The CORDEX framework. *World Meteorological Organization (WMO) Bulletin*, 58(3), 175.
- Goldstein, H., & Healy, M. J. R. (1995). The graphical presentation of a collection of means. *Journal of the Royal Statistical Society. Series A (Statistics in Society)*, 158(1), 175–177.
- Gutiérrez, J. M., Herrera, S., Cardoso, R. M., Soares, P. M. M., Espírito-Santo, F., & Viterbo, P. (2019). Iberia01: Daily gridded (0.1 resolution) dataset of precipitation and temperatures over the Iberian Peninsula. <https://doi.org/10.20350/digitalCSIC/8641>
- Gutirrez, J. M., Maraun, D., Widmann, M., Huth, R., Hertig, E., Benestad, R., et al. (2018). An intercomparison of a large ensemble of statistical downscaling methods over Europe: Results from the VALUE perfect predictor cross-validation experiment. *International Journal of Climatology*, 39, 3750–3785. <https://doi.org/10.1002/joc.5462>
- Gutowski Jr, W. J., Giorgi, F., Timbal, B., Frigon, A., Jacob, D., Kang, H.-S., et al. (2016). WCRP COordinated Regional Downscaling EXperiment (CORDEX): A diagnostic MIP for cMIP6. *Geoscientific Model Development*, 9(11), 4087–4095. <https://doi.org/10.5194/gmd-9-4087-2016>
- Haylock, M., Hofstra, N., Klein-Tank, A., Klok, E., Jones, P., & New, M. (2008). A European daily high-resolution gridded data set of surface temperature and precipitation for 1950–2006. *Journal of Geophysical Research*, 113, D20119. <https://doi.org/10.1029/2008JD010201>
- Herrera, S. (2011). PhD thesis: Desarrollo, validación y aplicaciones de Spain02: Una rejilla de alta resolución de observaciones interpoladas para precipitación y temperatura en España, in spanish (Ph.D. Thesis), Universidad de Cantabria.
- Herrera, S., Cardoso, R. M., Soares, P. M. M., Espírito-Santo, F., Viterbo, P., & Gutiérrez, J. M. (2019). Iberia01: A new gridded dataset of daily precipitation and temperatures over Iberia. *Earth System Science Data*, 11, 1947–1956. <https://doi.org/10.1007/s00382-014-2432-x>
- Herrera, S., Fernández, J., & Gutiérrez, J. M. (2015). Update of the Spain02 gridded observational dataset for EURO-CORDEX evaluation: Assessing the effect of the interpolation methodology. *International Journal of Climatology*, 36(2), 900–908. <https://doi.org/10.1002/joc.4391>
- Herrera, S., Gutiérrez, J. M., Ancell, R., Pons, M. R., Frías, M. D., & Fernández, J. (2012). Development and analysis of a 50-year high resolution daily gridded precipitation dataset over Spain (Spain02). *International Journal of Climatology*, 36, 74–85. <https://doi.org/10.1002/joc.2256>
- Hggmark, L., Ivarsson, K.-I., Gollvik, S., & Olofsson, P.-O. (2000). MESAN, an operational mesoscale analysis system. *Tellus A: Dynamic Meteorology and Oceanography*, 52(1), 2–20. <https://doi.org/10.3402/tellusa.v52i1.12250>
- Jacob, D., Petersen, J., Eggert, B., Alias, A., Christensen, O., Bouwer, L., et al. (2014). EURO-CORDEX: New high-resolution climate change projections for European impact research. *Regional Environmental Change*, 14(2), 563–578. <https://doi.org/10.1007/s10113-013-0499-2>
- Jerez, S., Montavez, J., Gomez-Navarro, J., Lorente-Plazas, R., Garcia-Valero, J., & Jimenez-Guerrero, P. (2013). A multi-physics ensemble of regional climate change projections over the Iberian Peninsula. *Climate Dynamics*, 41(7), 1749–1768. <https://doi.org/10.1007/s00382-012-1551-5>
- Julious, S. A. (2004). Using confidence intervals around individual means to assess statistical significance between two means. *Pharmaceutical Statistics*, 3(3), 217–222. <https://doi.org/10.1002/pst.126>
- Katragkou, E., García-Díez, M., Vautard, R., Sobolowski, S., Zanis, P., Alexandri, G., et al. (2015). Regional climate hindcast simulations within EURO-CORDEX: Evaluation of a WRF multi-physics ensemble. *Geoscientific Model Development*, 8, 603–618. <https://doi.org/10.5194/gmd-8-603-2015>
- Knist, S., Goergen, K., Buonomo, E., Christensen, O. B., Colette, A., Cardoso, R. M., et al. (2017). Land-atmosphere coupling in EURO-CORDEX evaluation experiments. *Journal of Geophysical Research: Atmospheres*, 122, 79–103. <https://doi.org/10.1002/2016JD025476>
- Kotlarski, S., Keuler, K., Christensen, O. B., Colette, A., Déqué, M., Gobiet, A., et al. (2014). Regional climate modeling on European scales: A joint standard evaluation of the EURO-CORDEX RCM ensemble. *Geoscientific Model Development*, 7(4), 1297–1333. <https://doi.org/10.5194/gmd-7-1297-2014>
- Kotlarski, S., Szabó, P., Herrera, S., Rty, O., Keuler, K., Soares, P. M., et al. (2017). Observational uncertainty and regional climate model evaluation: A pan-European perspective. *International Journal of Climatology*, 39, 3730–3749. <https://doi.org/10.1002/joc.5249>
- Lamb, H. (1972). *British isles weather types and a register of the daily sequence of circulation patterns 1861–1971*, Geophysical memoirs: H.M. Stationery Office.
- Laprise, R. (2008). Regional climate modelling. *Journal of Computational Physics*, 227(7), 3641–3666.
- Lopes, R. H. C. (2011). Kolmogorov-Smirnov test. In Lovric, M. (Ed.), *International encyclopedia of statistical science* (pp. 718–720). Berlin, Heidelberg: Springer Berlin Heidelberg. [https://doi.org/10.1007/978-3-642-04898-2\\_326](https://doi.org/10.1007/978-3-642-04898-2_326)
- Meehl, G., Stocker, T., Collins, W., Friedlingstein, P., Gaye, A., Gregory, J., et al. (2007). *Global climate projections*. Cambridge, United Kingdom and New York, NY, USA: Cambridge University Press.
- Mínguez, R., Tomás, A., Méndez, F. J., & Medina, R. (2013). Mixed extreme wave climate model for reanalysis databases. *Stochastic Environmental Research and Risk Assessment*, 27, 757–768. <https://doi.org/10.1007/s00477-012-0604-y>
- Moss, R., Edmonds, J., Hibbard, K., Manning, M., Rose, S., van Vuuren, D., et al. (2010). The next generation of scenarios for climate change research and assessment. *Nature*, 463, 747–56. <https://doi.org/10.1038/nature08823>
- Muñoz-Díaz, D., & Rodrigo, F. (2004). Spatio-temporal patterns of seasonal rainfall in Spain (1912–2000) using cluster and principal component analysis: Comparison. *Annales Geophysicae*, 22, 1435–1448. <https://doi.org/10.5194/angeo-22-1435-2004>

- Nikulin, G., Kjellstrom, E., Hansson, U., Strandberg, G., & Ullerstig, A. (2011). Evaluation and future projections of temperature, precipitation and wind extremes over Europe in an ensemble of regional climate simulations. *Tellus*, 63A, 41–55. <https://doi.org/10.1111/j.1600-0870.2010.00466.x>
- Randall, D., Wood, R., Bony, S., Colman, R., Fichefet, T., Fyfe, J., et al. (2007). *Climate models and their evaluation*. Cambridge, United Kingdom and New York, NY, USA: Cambridge University Press.
- Rios-Entenza, A., Soares, P. M. M., Trigo, R. M., Cardoso, R. M., & Miguez-Macho, G. (2014). Moisture recycling in the Iberian Peninsula from a regional climate simulation: Spatiotemporal analysis and impact on the precipitation regime. *Journal of Geophysical Research: Atmospheres*, 119, 5895–5912. <https://doi.org/10.1002/2013JD021274>
- Rummukainen, M. (2010). State-of-the-art with regional climate models. *Wiley Interdisciplinary Reviews: Climate Change*, 1(1), 82–96. <https://doi.org/10.1002/wcc.8>
- Soares, P. M. M., Cardoso, R. M., Ferreira, J. J., & Miranda, P. M. A. (2015). Climate change and the Portuguese precipitation: ENSEMBLES regional climate models results. *Climate Dynamics*, 45(7), 1771–1787. <https://doi.org/10.1007/s00382-014-2432-x>
- Soares, P. M. M., Cardoso, R. M., Lima, D. C. A., & Miranda, P. M. A. (2017). Future precipitation in Portugal: High-resolution projections using WRF model and EURO-CORDEX multi-model ensembles. *Climate Dynamics*, 49(7), 2503–2530. <https://doi.org/10.1007/s00382-016-3455-2>
- Soares, P. M. M., Cardoso, R. M., Miranda, P. M. A., de Medeiros, J., Belo-Pereira, M., & Espírito-Santo, F. (2012). WRF high resolution dynamical downscaling of ERA-Interim for Portugal. *Climate Dynamics*, 39(9), 2497–2522. <https://doi.org/10.1007/s00382-012-1315-2>
- Soares, P. M. M., Cardoso, R. M., Miranda, P. M. A., Viterbo, P., & Belo-Pereira, M. (2012). Assessment of the ENSEMBLES regional climate models in the representation of precipitation variability and extremes over Portugal. *Journal of Geophysical Research*, 117, D07114. <https://doi.org/10.1029/2011JD016768>
- Trigo, R. M., & DaCamara, C. C. (2000). Circulation weather types and their influence on the precipitation regime in Portugal. *International Journal of Climatology*, 20(13), 1559–1581. [https://doi.org/10.1002/1097-0088\(20001115\)20:13<1559::AID-JOC555>3.0.CO;2-5](https://doi.org/10.1002/1097-0088(20001115)20:13<1559::AID-JOC555>3.0.CO;2-5)
- Turco, M., Palazzi, E., Hardenberg, J., & Provenzale, A. (2015). Observed climate change hotspots. *Geophysical Research Letters*, 42, 3521–3528. <https://doi.org/10.1002/2015GL063891>
- van der Linden, P., & Mitchell, J. F. B. (Eds.) (2009). *ENSEMBLES: Climate change and its impacts: Summary of research and results from the ENSEMBLES project Edited by van der Linden, P., & Mitchell, J. F. B.* FitzRoy Road, Exeter EX1 3PB, UK: Met Office Hadley Centre.
- Viceto, C., Marta-Almeida, M., & Rocha, A. (2017). Future climate change of stability indices for the Iberian Peninsula. *International Journal of Climatology*, 37(12), 4390–4408. <https://doi.org/10.1002/joc.5094>